

# Experimental Study of Odor Source Localization on a Mobile Robot

Lingxiao Wang<sup>1</sup>, Ziyu Yin<sup>2</sup>, and Shuo Pang<sup>2</sup>

**Abstract**—Autonomous odor source localization (OSL) is a technology that enables robots to locate odor sources in unknown environments. Designing an effective olfactory-based navigation algorithm, which guides the robot to detect odor plumes as cues and trace back to the odor source, is the key to correctly finding the odor source. Recently, we published three olfactory-based navigation algorithms, namely moth-inspired, adaptive moth-inspired, and reinforcement learning-based algorithms. Previous studies presented each algorithm’s simulation results, but their search performance in on-vehicle tests is unknown. This paper aims to adapt three navigation algorithms from the simulation program into real-world environments. We modified three algorithms to fit the real-world settings and tested different parameter values to find the best fit. Moreover, we compared three algorithms in different airflow environments to evaluate their performance in on-vehicle tests. Experiment results show that the adaptive moth-inspired algorithm achieves the best performance in laminar airflow environments in terms of the averaged search time and success rate. In contrast, the RL-based algorithm outperforms the others in turbulent airflow environments.

## I. INTRODUCTION

Olfaction is an important sensing ability that is widely used by animals to perform life-essential activities, such as homing, foraging, mate-seeking, and evading predators. Inspired by olfactory behaviors of animals, a mobile robot or an autonomous vehicle, equipped with odor detection sensors (e.g., chemical sensors), could locate an odor source in an unknown environment. The technology of employing robots to find odor sources is referred to as odor source localization (OSL) [1]. Some practical OSL applications include monitoring air pollution [2], locating chemical gas leaks [3], locating unexploded mines and bombs [4], and marine surveys such as finding hydrothermal vents [5].

To correctly find an odor source, an effective olfactory-based navigation algorithm is critical. Like image-based navigation algorithms, which utilize the information extracted from images as references to navigate a robot, olfactory-based navigation algorithms detect odor plumes as cues to guide a robot in finding the odor source. The challenging part of this navigation problem is to estimate the emitted odor plume locations, which are not only related to the molecular diffusion that takes plumes away from the odor source but also the advection of airflows [6].

In laminar flow environments, plume dispersal is a steady and stable process, which results in a spatially coherent

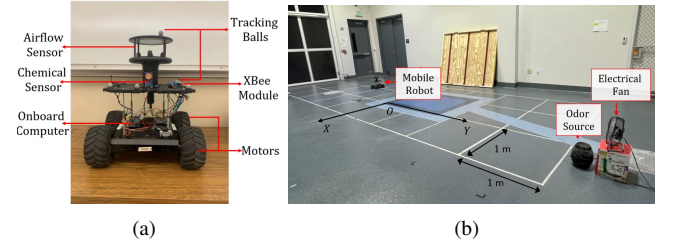


Fig. 1. (a) The mobile robot used in this work. This robot is equipped with an airflow sensor for measuring wind speeds and directions; a chemical sensor for detecting odor plumes; Xbee modules for wireless communication; an onboard computer for processing sensor data. (b) The experiment setup. The robot is initially placed at downwind area with the object of finding the odor source. A humidifier loaded with ethanol is employed to generate odor plumes, and an electrical fan is placed behind the humidifier to create an artificial wind field.

plume trajectory. In this scenario, the intuitive gradient following algorithm, i.e., chemotaxis [7], is applicable for guiding a robot to find the odor source. However, in a turbulent flow environment, odor plumes are stretched and twisted to form an intermittent concentration trajectory, which fails the chemotaxis in this environment. Alternatively, two other categories of olfactory-based navigation algorithms, namely bio-inspired and engineering-based (i.e., probabilistic) algorithms, have been proposed [8].

A bio-inspired algorithm directs the robot to mimic animal odor search behaviors. A typical bio-inspired algorithm is the moth-inspired method, which imitates the mate-seeking behaviors of male moths [9]: a male moth flies upwind when detecting pheromone plumes and across the wind when plumes are absent. This behavior can be framed as a ‘surge/casting’ model [10], where a plume tracing robot moves against the wind direction when detecting plumes (i.e., ‘surge’) and traverses wind when missing plume contact (i.e., ‘casting’). By contrast, engineering-based navigation algorithms utilize mathematical and physics-based approaches to deduce possible odor source locations. Then, a path planner is employed to direct the robot to the estimated target.

Recently, we published three olfactory-based navigation algorithms, including moth-inspired [11], adaptive moth-inspired [12], and reinforcement learning (RL)-based navigation algorithms [13]. Simulation results were presented in previous studies, but their real-world performance needed further investigation. This paper presents experimental studies of the aforementioned navigation algorithms in real-world search environments. Contributions of this work can be summarized as: 1) adapt three recently published olfactory-based navigation algorithms from the simulated into real-world environments; 2) evaluate different parameter values

<sup>1</sup>Lingxiao Wang is with Electrical Engineering Department, Louisiana Tech University, Ruston, LA 71272, USA [lwang@latech.edu](mailto:lwang@latech.edu)

<sup>2</sup>Ziyu Yin and Shuo Pang are with Electrical Engineering and Computer Science Department, Embry-Riddle Aeronautical University, Daytona Beach, FL 32114, USA [yinz@my.erau.edu](mailto:yinz@my.erau.edu), [shuo.pang@erau.edu](mailto:shuo.pang@erau.edu)

to find the best fit; 3) compare search performance of these algorithms in different real-world search environments. Besides, experiment results of this work can also inspire the design of new olfactory-based navigation algorithms. For instance, by evaluating the search performance of these navigation algorithms in different airflow environments, we can design an adaptive navigation algorithm that can alter its search strategy depending on changes in airflow environments.

The robotic platform and experiment field are presented in Fig. 1. A mobile robot was build as the robotic platform, and the search area contains an odor source, where the odor source location is unknown to the robot. In the remaining of this paper, Section II reviews the recent progress of olfactory-based navigation algorithms; Section III reviews technical details of the implemented olfactory-based navigation algorithms; Section IV presents experiment details of performing the on-vehicle tests.

## II. RELATED WORKS

Early works of robotic OSL attempt to complete this task via a simple gradient following algorithm, i.e., chemotaxis. A common implementation of this algorithm is to install a pair of chemical sensors on the left and right sides of a plume-tracing robot, where the robot is commanded to steer to the side with the higher concentration measurement [14]. Many research works [15], [16], [17], [18] have proved the validity of chemotaxis in laminar flow environments (i.e., low Reynolds numbers).

In turbulent flow environments (i.e., high Reynolds numbers), bio-inspired and engineering-based methods were proposed to solve the OSL problem. Bio-inspired methods direct robots to find the odor source via imitating animals' odor search behaviors. Lochmatter *et al.* [19] implemented the moth-inspired method on a mobile robot to find an odor source in a laminar flow environment. Li *et al.* [20] applied a moth-inspired method on an autonomous underwater vehicle (AUV) to find an underwater chemical source over a large search area. Above the ground, Luo *et al.* [21] designed a flying odor compass on an unmanned aerial vehicle (UAV), which can identify the airflow direction based on plume detection events and find the odor source accordingly.

The 'surge/casting' model in the moth-inspired methods can be modified to improve the search performance. Farrell *et al.* [11] added 'track-in' and 'track-out' behaviors in the 'surge' phase to increase the plume contact duration. Shigaki *et al.* [22] presented a time varying moth-inspired method, where the duration of the 'surge' behavior is controlled via an equation obtained from observations of biological experiments. In [23], Shigaki *et al.* designed a fuzzy controller to adaptively adjust the transition among different behaviors according to airflow changes. For the 'casting' behavior, Ferri *et al.* [24] proposed a 'spiral' trajectory, and Rahbar *et al.* [25] presented a 3-dimensional (3-D) version 'spiral' trajectory with the real-world validation. Many other bio-inspired search strategies, such as zigzag [26] and multi-phase exploratory [27], have been proposed based on the

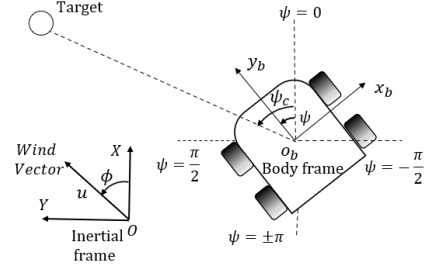


Fig. 2. Robot notations. Wind speed  $u$  and wind direction  $\phi$  are measured from the onboard anemometer in the inertial frame. Robot position  $(x, y)$  and heading  $\psi$  are monitored by the indoor localization system.

'surge/casting' behavior model.

Engineering-based methods, on the other hand, navigate a robot relying on odor source estimations. A common way to indicate the odor source distribution is constructing a source probability map. This map divides the search area into multiple small regions and assigns every region with a probability value, indicating how likely this region contains the odor source. The Bayesian-inference method [28] is a typical engineering-based OSL algorithm, which formulates the plume propagation as a Gaussian random process. Based on a series of plume detection and non-detection events, the robot can inversely calculate the probability of a region containing the odor source. Other source mapping algorithms include particle filter [29], hidden Markov model (HMM) [30], occupancy grid mapping [31], source term estimation [32], [33], and partially observable Markov decision process (POMDP) [34]. The core idea of these methods is to perceive the environment (especially airflow information) and estimate possible odor source locations accordingly.

After a source probability map is obtained, the robot is commanded to move toward the estimated source location (i.e., the area with the highest probability of containing the odor source) via a path planning algorithm. Possible path planners include the artificial potential field (APF) [35] and A-star [36] algorithms. Besides, Vergassola *et al.* [37] proposed the 'infotaxis' algorithm, which uses the information entropy to guide the robot searching for the odor source. In this method, the robot selects a future movement that mostly reduces the information uncertainty of the odor source.

## III. METHODOLOGY

### A. Description of an OSL Task

An OSL task can be separated into three search phases, namely plume finding, plume tracing, and source declaration [38]. The first phase, i.e., plume finding, aims to verify the existence of plumes in the search area. After the robot detects plumes for the first time, the plume tracing phase is activated, in which the robot detects plumes as cues to approach the odor source. Once the robot is close to the source location, it identifies the odor source (e.g., via onboard cameras) and declares the source location in the source declaration phase, which is also considered as the end of an OSL task.

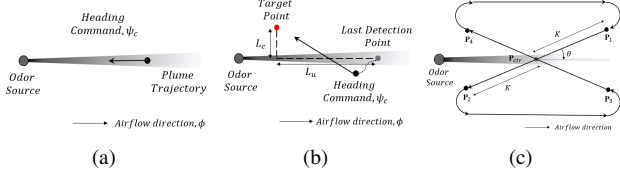


Fig. 3. Moth-inspired search behaviors. (a) ‘Track-in’ behavior. (b) ‘Track-out’ behavior. To traverse the plume trajectory, the robot moves to a target point (red dot).  $L_u$  and  $L_c$  are horizontal and vertical distances from the target point to the last detection point. (c) ‘Reacquire’ behavior. The center point (i.e.,  $P_{ctr}$ ) is the last detection point. The distance from  $P_{ctr}$  to a corner point (i.e.,  $P_1$  to  $P_4$ ) is  $K$  and the angle difference is  $\theta$ . The robot will reach each corner point in an ascending order to complete a ‘Bow-tie’.

In this work, the OSL is considered as a 2-dimensional (2-D) search problem since the implemented robotic agent is a mobile robot. As presented in Fig. 2, the robot measures odor concentrations  $\rho$ , wind speeds  $u$  and directions  $\phi$  in the inertial frame, robot heading  $\psi$ , and robot positions  $(x, y)$  during the plume tracing process. Sensor readings are fed to the implemented olfactory-based navigation algorithm to calculate robot heading commands. The robot moves in a constant speed to simplify the control problem, and an OSL task is considered as success if the robot is in the vicinity of the odor source.

### B. Review of Three Implemented Olfactory-based Navigation Algorithms

1) *Moth-inspired Method*: The moth-inspired method [11] can be summarized as the alternation of ‘surge’ and ‘casting’ behaviors. The implemented moth-inspired method further divides the ‘surge’ behavior into ‘track-in’ and ‘track-out’ behaviors and models the ‘casting’ behavior as a ‘bow-tie’ search trajectory as presented in Fig. 3.

In the ‘track-in’ behavior, the robot moves upwind to make a rapid progress toward the odor source while plumes have been detected. When the robot moves out of plumes, the ‘track-out’ behavior is activated to manipulate the robot to traverse the plume trajectory. The hope is that the robot can encounter plumes via this behavior, but if it does not, then the ‘reacquire’ behavior is activated, which commands the robot to perform crosswind excursions to re-detect plumes over a wide region. Once the robot detects plumes, it turns back to the ‘track-in’ behavior. These search behaviors repeat until the robot finds the odor source.

2) *Adaptive Moth-inspired Method*: In the moth-inspired method, parameters in search behaviors, like  $L_c$ ,  $L_u$ ,  $K$ , and  $\theta$ , govern the scale of robot search routes (see Fig. 3). In the traditional moth-inspired method [11], these parameters are determined by trial and error prior to an OSL task, and their values are fixed during the entire search. An improved design is to dynamically adjust search parameters according to the current search situation. For instance, when the airflow becomes turbulent, large parameter values (e.g.,  $L_u$ ,  $K$ , and  $\theta$ ) are preferred to generate an oscillating trajectory for detecting meandering plumes over a wide range, while small values are desired to produce a smooth path in a laminar flow environment, facilitating the robot to maintain inside plumes.

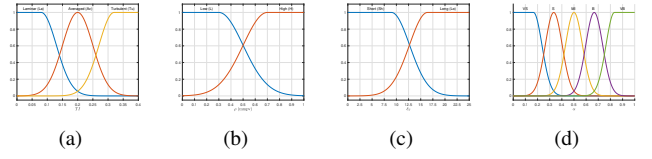


Fig. 4. Membership functions and fuzzy sets for inputs and output of the fuzzy controller proposed in the adaptive moth-inspired method. Inputs include: (a) turbulence intensity  $TI$  with 3 fuzzy sets: ‘laminar’, ‘average’, and ‘turbulent’; (b) sensed odor concentration  $\rho$  with 2 fuzzy sets: ‘low’ and ‘high’; (c) plume non-detection period  $\delta_T$  with 2 fuzzy sets: ‘short’ and ‘long’. The output is (d), which represents coefficients of behavior parameters, i.e.,  $\alpha_{L_u}, \dots, \alpha_{\theta}$ . Five fuzzy sets are defined for an output: ‘very small’, ‘small’, ‘middle’, ‘big’, and ‘very big’.

Specifically, a fuzzy controller is designed to estimate the current search situation and change parameter values accordingly. Three fuzzy inputs are employed to estimate the current search situation, including turbulent intensity (i.e.,  $TI$ ), sensed odor concentration (i.e.,  $\rho$ ), and plume non-detection period (i.e.,  $\delta_T$ ). Specifically,  $TI$  can be calculated from the sensed airflow history via  $TI = \mu/\sigma$  [39], where  $\mu$  and  $\sigma$  are the mean and the standard deviation of the recorded airflow history, respectively. High  $TI$  values indicate the robot is in a turbulent flow environment, and vice versa. In this work, the length of recorded airflow history ( $H$ ) is defined as 40, i.e.,  $TI$  is calculated based on previous 40 airflow measurements. We tested different values of  $H$  and found that longer  $H$  results in a sluggish  $TI$  change, i.e.,  $TI$  cannot timely reflect airflow changes in the search environment.

Outputs of the fuzzy controller are a group of coefficients (range from 0 to 1) that adjust parameter values, including  $\alpha_{L_u}$ ,  $\alpha_{L_c}$ ,  $\alpha_K$ , and  $\alpha_{\theta}$ . Each coefficient is applied on a base value, e.g.,  $L_u = \alpha_{L_u} \cdot L_{u,base}$ . Therefore, by varying values of coefficients, parameter values will change correspondingly. The selection of base values can be determined based on the size of search area and the robot moving speed. In this work, base values of  $L_u$ ,  $L_c$ ,  $K$ , and  $\theta$  are 1.5 m, 1.5 m, 2 m, and 45 degrees, respectively.

Fig. 4 presents membership functions and fuzzy sets for inputs and outputs of the designed fuzzy controller. The Gaussian membership function is selected for all fuzzy sets. Fuzzy rules are designed in such a way: when the robot is in a turbulent environment,  $L_c$ ,  $K$ , and  $\theta$  are increased to extend crosswind excursions, improving the probability of detecting plumes in larger areas; when the airflow becomes laminar or the robot is close to the odor source,  $L_u$  is increased to enhance the upwind movements, leading the robot to quickly approach the odor source location.

3) *RL-based Method*: The RL-based method [13] models the OSL as an RL problem, where the agent is modeled as the plume-tracing robot and the environment is modeled as the search area. By properly designing reward functions, the agent is stipulated to choose actions that benefit in finding the odor source location. The key is to define reward functions so that the robot is encouraged to find the odor source.

Fig. 5 shows the principle of RL-based method. Specifi-

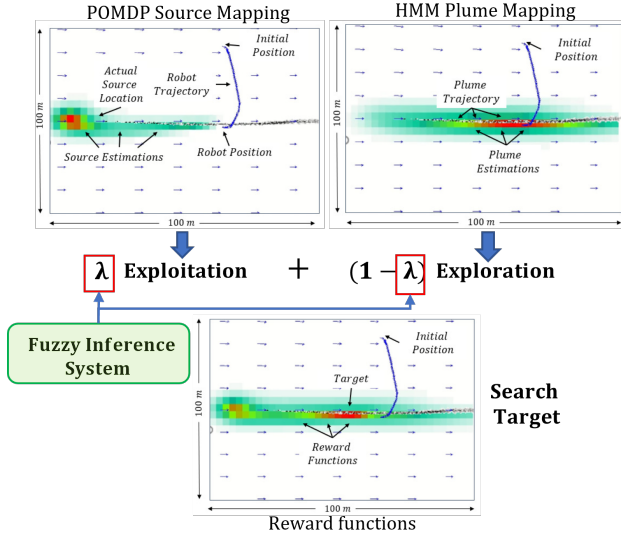


Fig. 5. The structure of the RL-based method. POMDP source mapping algorithm generates a source probability map, indicating areas of containing the odor source (red areas). HMM plume mapping algorithm produces a plume likelihood map, estimating possible plume distribution areas (red areas). Two maps are weighted combined by using a fuzzy inference system to calculate reward functions, where the red area is the current search target.

cally, this method contains two principal procedures, namely modeling and planning. In the modeling procedure, the robot estimates possible odor source and plume locations. Belief states in a partially observable Markov decision process (POMDP) are adapted to represent a source probability map, which indicates the probability of each region in the search area containing the odor source. For odor plume estimates, a hidden Markov model (HMM)-based plume mapping algorithm is adopted to generate a plume distribution map, indicating the likelihood of a region containing the odor plume. Then, a fuzzy inference system is designed to fuse the information from two maps to calculate reward function. If the robot is close to the odor source, the fuzzy inference system emphasizes source estimates in reward function, enabling the robot to move to the source estimate. In contrast, the fuzzy inference system puts more weight on plume estimates in reward function, enabling the robot to detect odor plumes and to improve the reliability of source estimates.

Finally, search routes are determined based on the generated reward functions in the planning procedure. The value iteration method is adopted to solve the RL problem and produces the optimal policy, which is a search route that leads the robot to the maximum reward location, i.e., the location that contains the most odor source information. Modeling and planning procedures alternate until reward functions converge, which is considered as the complete of an OSL problem.

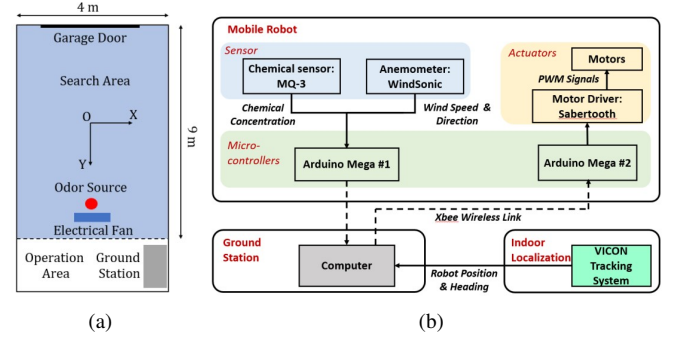


Fig. 6. (a) Search area (b) System configuration. This system contains three main components, including mobile robot, ground station, and indoor localization system. The solid connection line represents physical cables, and the dotted connection line represents wireless link.

## IV. EXPERIMENTS

### A. Experiment Setup

Experiments were conducted in the Indoor Autonomous Robots Testing Lab at the Embry-Riddle Aeronautical University. We divide the lab into two areas, including a search area where the robot can move and an operation area for accommodating the ground station. As shown in Fig. 6(a), the size of the search area is  $9 \times 4 \text{ m}^2$ , containing an odor source. The ethanol vapor was employed as the odor source since it is minimally toxic and commonly implemented in OSL research [40]. To accelerate the odor dispersion, ethanol was put in a humidifier to consistently release odor plumes, and an electric fan was placed behind the odor source to accelerate the odor propagation.

Fig 6(b) shows the configuration of the designed robotic system, which includes three main components, namely a mobile robot, a ground station, and an indoor localization system. The mobile robot is equipped with a chemical sensor (MQ-3, Waveshare) and an anemometer (WindSonic, Gill Instruments). Both sensors are connected to a micro-controller (Arudino Mega, Arduino) for fetching sensor measurements. The second onboard micro-controller controls robot motors via a motor driver (Sabertooth, Dimension Engineering). Two micro-controllers can communicate with the ground station via a wireless communication network, comprising multiple Xbee modules (Xbee, Digi international). The camera tracking system (Vicon, Vicon Inc.) is employed to determine indoor positions, which sends robot positions and orientations to the ground station via an Ethernet cable. The update frequency of navigation algorithms was set to 4 Hz.

Since the chemical sensor has a long recovery time, an adaptive concentration threshold [29] is employed to determine the odor detection and non-detection events. During an OSL test, the robot sends sensor measurements to the ground station, where the navigation algorithm calculates robot's heading commands based on onboard sensor measurements. Then, commands will be transmitted back to the mobile robot via the wireless communication network. The robot moves toward the target heading and collects information at the new location. The transmission time between the robot



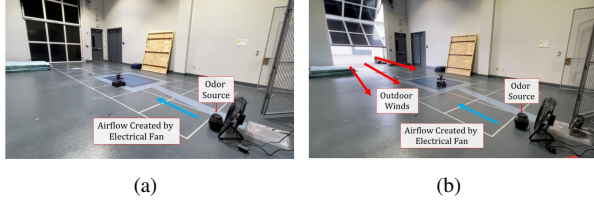


Fig. 7. Two airflow conditions. (a) Laminar airflow environment. The garage door is closed, creating an enclosed search space. The main airflow direction is created by the electrical fan. (b) Turbulent airflow environment. The garage door is opened, allowing outdoor winds blowing inside the search area.

and ground station is negligible due to the short transmission distance. These processes repeat until the robot finds the odor source, i.e., the distance between the odor source and robot is less than 0.5 m (this radius is determined based on the size of the robot and the size of search area). In the ground station, the MATLAB software was employed to implement olfactory-based navigation algorithms and read data from onboard sensors and the indoor localization system.

### B. Experiment Design

To evaluate the performance of the aforementioned navigation methods, around 60 tests have been conducted in both laminar and turbulent airflow environments. As shown in Fig 7(a), in the laminar flow environment, the main airflow field is generated by the electrical fan. To create a turbulent airflow field, the garage door at the back of the lab is opened as presented in Fig 7(b), allowing outdoor winds blowing into the search area to create a turbulent airflow environment.

All tests can be separated into three groups. In group 1, three navigation methods were implemented in a laminar flow environment to verify their validities. Tests in group 2 and 3 were carried out to investigate the robustness of navigation methods. Specifically, the robot was placed at different initial positions in group 2 tests, while in group 3, each navigation algorithm was repeated performed in both laminar and turbulent airflow environments. In these tests, search times and robot search trajectories were recorded and compared.

### C. Group 1: Verification of Three Navigation Methods

In this group of tests, the robot starts at the same initial position and moves in the same speed, i.e., 0.15 m/s. Fig. 8 presents robot search trajectories. It can be observed that the robot can correctly find the odor source with three navigation methods, i.e., the robot arrives the odor source location at the end of the search.

Specifically, Fig. 9 presents snapshots of the robot directed by the moth-inspired navigation method. At the beginning of the search (i.e., from  $t = 1$  to 15 s), the robot alternates between the ‘track-in’ and ‘track-out’ behavior and moves upwind. At  $t = 30$  s, the robot loses plume contact and performs the ‘reacquire’ behavior. The robot re-detects plumes at  $t = 47$  s and turns back to the ‘track-in’ behavior at  $t = 50$  s. The robot continuously detects plumes and correctly finds the odor source at  $t = 58$  s. The travel distance is 8.76 m.

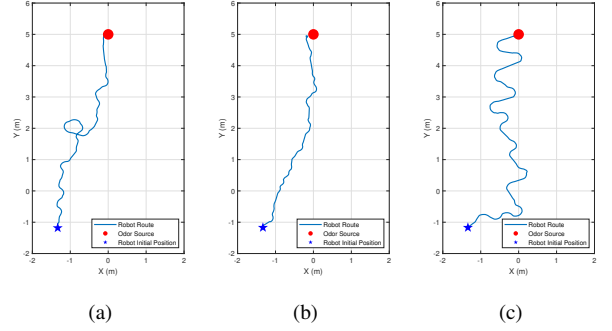


Fig. 8. Sample runs of three algorithms in Group 1 tests. The blue star indicates the robot initial position  $(-1.3, -1.2)$  m, and red dot is the odor source location  $(0, 5)$  m. (a) Moth-inspired method. Search time: 58 s; travel distance: 8.76 m (b) Adaptive moth-inspired method. Search time: 43 s; travel distance: 6.92 m (c) RL-based method. Search time: 75 s; travel distance: 10.81 m.

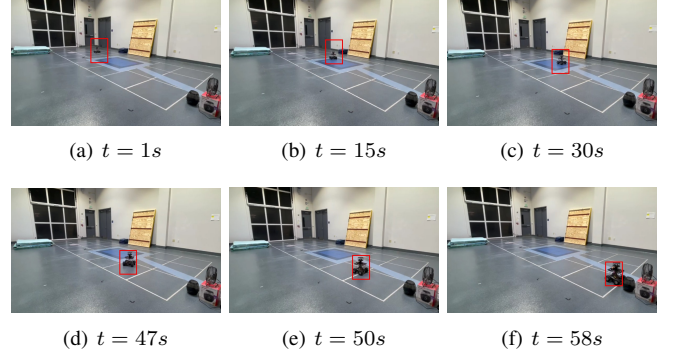


Fig. 9. Snapshots of an OSL test with the moth-inspired method. The robot position is highlighted with the a red rectangle, and the robot correctly finds the odor source at 58 s.

Fig. 10 shows plots of inputs and outputs of the fuzzy controller in the adaptive moth-inspired method. It can be seen that behavior parameters can adaptively change according to different search situations: when the robot is far from the odor source and the estimated airflow characteristic is turbulent (i.e.,  $t = 5$  s), values of  $L_c$ ,  $K$ , and  $\theta$  are large to emphasize cross-wind movements to increase the probability of detecting plumes; when the robot is near to the odor source (i.e.,  $t = 42$  s), values of  $L_u$  is increased, improving the upwind movement. The robot finds the odor source at 43 s and travels 6.92 m.

As for the RL-based method, Fig. 11 presents the source probability map, plume distribution map, and the fused reward map. The size of a sub-region in these maps is  $0.5 \times 0.5$  m<sup>2</sup>, which is comparable to the size of the mobile robot. When  $t = 20$  s, the fusion coefficient (i.e., the output of the fuzzy inference system) is 0.8, which emphasizes the plume distribution map in the reward map. Thus, the robot tends to find plumes to collect more odor source information instead of chasing the source estimate. When  $t = 70$  s, the fusion coefficient becomes 0.2, directing the robot to move toward the source estimate  $(0, 4.5)$  m (the actual odor source is at  $(0, 5)$  m). The robot reaches the odor source location

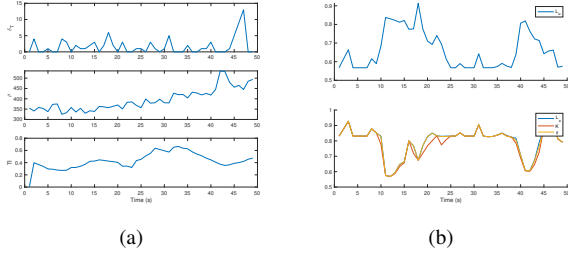


Fig. 10. Fuzzy inputs and outputs of the implemented fuzzy controller in the adaptive moth-inspired method. (a) Fuzzy inputs include plume non-detection period  $\delta_T$ , odor concentration  $\rho$ , and turbulent intensity  $TI$ . (b) Fuzzy outputs are coefficients that adjust search behaviors, including  $L_u$  (on the top plot),  $L_c$ ,  $K$ , and  $\theta$  (on the bottom plot).

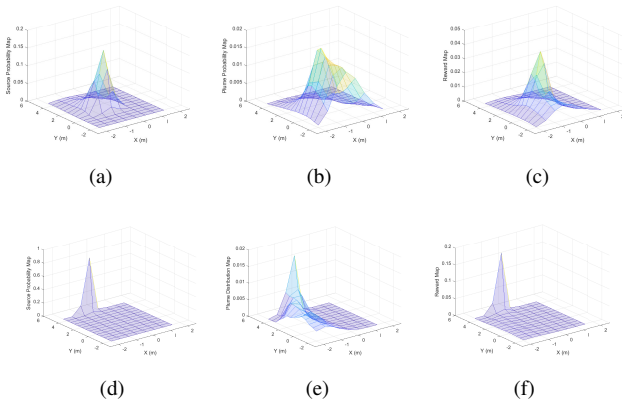


Fig. 11. Results from the source mapping, plume mapping, and fusion algorithms in the RL-based method. The first row of diagrams, i.e., (a), (b), and (c), shows the source probability map, plume distribution map, and reward map at  $t = 20$  s, respectively. The second row of diagrams, i.e., (d), (e), and (f), shows the aforementioned maps at  $t = 70$  s.

when  $t = 75$  s, and the travel distance is 10.81 m.

#### D. Group 2: Different Robot Initial Positions

In this group of tests, the robot was placed at three different initial positions, including left, middle, and right positions, in the laminar flow environment. Fig. 12 shows robot search trajectories with three navigation methods. It can be seen that all search trajectories terminates at the actual odor source location, i.e., no matter how the robot initial position changes, the robot can correctly find the odor source with three navigation methods.

#### E. Group 3: Repeat Tests in Different Airflow Environments

In this group of tests, three navigation methods were repeated performed in both laminar and turbulent airflow environments. The robot starts from the same initial position  $(-1, 0)$  m and moves in the same speed, i.e., 0.15 m/s.

Table I presents search time of three navigation methods in the laminar flow environment. It can be observed that the moth-inspired and adaptive moth-inspired methods outperform the RL-based method in most tests. This is because the simple ‘surge/casting’ behavior pattern is effective to quickly bring the robot close to the odor source in the laminar flow environment, while the RL-based method needs more time

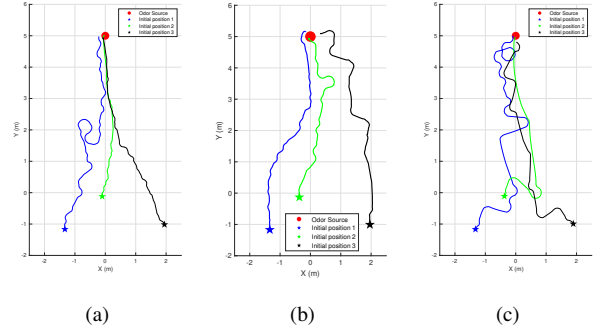


Fig. 12. Robot search trajectories starting at different initial positions. (a) Moth-inspired method. (b) Adaptive moth-inspired method. (c) RL-based method.

TABLE I  
SEARCH TIME OF THREE NAVIGATION METHODS IN THE LAMINAR FLOW ENVIRONMENT.  $\mu$ : MEAN SEARCH TIME;  $\sigma$ : STANDARD DEVIATION OF SEARCH TIME;  $f$ : SUCCESS RATE

	Moth-inspired Method (s)	Adaptive Moth-inspired Method (s)	RL-based Method (s)
Test 1	54	45	63
Test 2	56	42	68
Test 3	45	41	64
Test 4	40	40	63
Test 5	48	41	52
Test 6	42	41	65
Test 7	40	40	55
Test 8	44	46	52
Test 9	42	52	59
Test 10	53	41	54
$\mu$ (s)	46.4	<b>42.9</b>	59.5
$\sigma$	6.0	<b>3.8</b>	5.9
$f$	100%	<b>100%</b>	100%

to correctly compute source and plume estimates based on the sensed airflow history. When the robot loses the plume contact, the ‘reacquire’ behavior guides the robot to search plumes in nearby areas, and the robot has a high probability to re-detect plumes due to the steady and stable plume distribution in the laminar flow environment. Moreover, the adaptive moth-inspired method achieves a better performance than the original moth-inspired counterpart since the implemented fuzzy controller can dynamically adjust behavior parameters to fit different search situations, improving the search efficiency.

Search results in the turbulent flow environment are presented in Table II. Compared three navigation methods, both moth-inspired and adaptive moth-inspired methods fail to find the odor source in Test 4, while the RL-based method succeeds in all tests and achieves the shortest averaged search time 59.5 s. In turbulent airflows, the moth-inspired methods can hardly keep the robot maintaining inside plumes due to two reasons: 1) plumes are scratched by turbulent airflows to form an intermittent trajectory, deteriorating the performance of the ‘surge’ and ‘casting’ behaviors; 2) the decision (i.e., heading command) is made via the instantaneous airflow

TABLE II  
SEARCH TIME OF THREE NAVIGATION METHODS IN THE TURBULENT  
FLOW ENVIRONMENT.  $\mu$ : MEAN SEARCH TIME;  $\sigma$ : STANDARD  
DEVIATION OF SEARCH TIME;  $f$ : SUCCESS RATE

	Moth-inspired Method (s)	Adaptive Moth- inspired Method (s)	RL-based Method (s)
Test 1	60	48	55
Test 2	63	93	53
Test 3	71	38	66
Test 4	-	-	55
Test 5	63	103	65
Test 6	66	90	57
Test 7	85	81	90
Test 8	38	63	76
Test 9	116	75	54
Test 10	108	50	63
$\mu$ (s)	87.0	84.1	<b>59.5</b>
$\sigma$	46.0	46.0	<b>11.8</b>
$f$	90%	90%	<b>100%</b>

-: Fail to locate the source within 200 s.

measurements, which vary significantly and could lead the robot to the wrong directions. By contrast, the RL-based method can calculate source and plume estimates based on the recorded airflow history, which is more reliable than the instantaneous measurements.

## V. CONCLUSION AND FUTURE WORKS

This paper presents the experimental studies of three olfactory-based navigation methods, namely moth-inspired, adaptive moth-inspired, and RL-based methods. Three navigation methods were implemented in both laminar and turbulent flow environments to evaluate their validities. A mobile robot is constructed as the robotic platform to implement navigation methods. Experiment results show that in terms of the averaged search time and success rate, the adaptive moth-inspired method has the best search performance in the laminar flow environment, whereas the RL-based method outperforms the others in the turbulent flow environment.

Experiment results obtained in this work inspire the fusion of bio-inspired and engineering-based methods. In the future, we plan to design an olfactory-based navigation method that combines merits of bio-inspired and engineering-based methods: when the robot is in a laminar flow environment, the bio-inspired method controls the robot to swiftly approach the odor source, and when the airflow becomes turbulent or the robot is near to the odor source, the engineering-based method switches over to control the robot to find the odor source to improve the search efficiency.

## REFERENCES

- [1] G. Kowadlo and R. A. Russell, "Robot odor localization: a taxonomy and survey," *The International Journal of Robotics Research*, vol. 27, no. 8, pp. 869–894, 2008.
- [2] M. Dunbabin and L. Marques, "Robots for environmental monitoring: Significant advancements and applications," *IEEE Robotics & Automation Magazine*, vol. 19, no. 1, pp. 24–39, 2012.
- [3] S. Soldan, G. Bonow, and A. Kroll, "Robogasinpector-a mobile robotic system for remote leak sensing and localization in large industrial environments: Overview and first results," *IFAC Proceedings Volumes*, vol. 45, no. 8, pp. 33–38, 2012.
- [4] R. A. Russell, "Robotic location of underground chemical sources," *Robotica*, vol. 22, no. 1, pp. 109–115, 2004.
- [5] G. Ferri, M. V. Jakuba, and D. R. Yoerger, "A novel method for hydrothermal vents prospecting using an autonomous underwater robot," in *2008 IEEE International Conference on Robotics and Automation*. IEEE, 2008, pp. 1055–1060.
- [6] J. A. Farrell, J. Murlis, X. Long, W. Li, and R. T. Cardé, "Filament-based atmospheric dispersion model to achieve short time-scale structure of odor plumes," *Environmental fluid mechanics*, vol. 2, no. 1-2, pp. 143–169, 2002.
- [7] H. Ishida, K.-i. Suetsugu, T. Nakamoto, and T. Moriizumi, "Study of autonomous mobile sensing system for localization of odor source using gas sensors and anemometric sensors," *Sensors and Actuators A: Physical*, vol. 45, no. 2, pp. 153–157, 1994.
- [8] X.-x. Chen and J. Huang, "Odor source localization algorithms on mobile robots: A review and future outlook," *Robotics and Autonomous Systems*, vol. 112, pp. 123–136, 2019.
- [9] R. T. Cardé and A. Mafra-Neto, "Mechanisms of flight of male moths to pheromone," in *Insect pheromone research*. Springer, 1997, pp. 275–290.
- [10] L. L. López, V. Vouloutsis, A. E. Chimeno, E. Marcos, S. B. i Badia, Z. Mathews, P. F. Verschure, A. Ziyatdinov, and A. P. i Lluna, "Moth-like chemo-source localization and classification on an indoor autonomous robot," in *On Biomimetics*. IntechOpen, 2011.
- [11] J. A. Farrell, S. Pang, and W. Li, "Chemical plume tracing via an autonomous underwater vehicle," *IEEE Journal of Oceanic Engineering*, vol. 30, no. 2, pp. 428–442, 2005.
- [12] L. Wang and S. Pang, "Robotic odor source localization via adaptive bio-inspired navigation using fuzzy inference methods," *Robotics and Autonomous Systems*, vol. 147, p. 103914, 2022.
- [13] L. Wang, S. Pang, and J. Li, "Olfactory-based navigation via model-based reinforcement learning and fuzzy inference methods," *IEEE Transactions on Fuzzy Systems*, vol. 29, no. 10, pp. 3014–3027, 2021.
- [14] G. Sandini, G. Lucarini, and M. Varoli, "Gradient driven self-organizing systems," in *Proceedings of 1993 IEEE/RSJ International Conference on Intelligent Robots and Systems (IROS'93)*, vol. 1. IEEE, 1993, pp. 429–432.
- [15] F. W. Grasso, T. R. Consi, D. C. Mountain, and J. Atema, "Biomimetic robot lobster performs chemo-orientation in turbulence using a pair of spatially separated sensors: Progress and challenges," *Robotics and Autonomous Systems*, vol. 30, no. 1-2, pp. 115–131, 2000.
- [16] R. A. Russell, A. Bab-Hadiashar, R. L. Shepherd, and G. G. Wallace, "A comparison of reactive robot chemotaxis algorithms," *Robotics and Autonomous Systems*, vol. 45, no. 2, pp. 83–97, 2003.
- [17] A. Lilienthal and T. Duckett, "Experimental analysis of gas-sensitive Braitenberg vehicles," *Advanced Robotics*, vol. 18, no. 8, pp. 817–834, 2004.
- [18] H. Ishida, G. Nakayama, T. Nakamoto, and T. Moriizumi, "Controlling a gas/odor plume-tracking robot based on transient responses of gas sensors," *IEEE Sensors Journal*, vol. 5, no. 3, pp. 537–545, 2005.
- [19] T. Lochmatter, X. Raemy, L. Matthéy, S. Indra, and A. Martinoli, "A comparison of casting and spiraling algorithms for odor source localization in laminar flow," in *2008 IEEE International Conference on Robotics and Automation*. IEEE, 2008, pp. 1138–1143.
- [20] W. Li, J. A. Farrell, S. Pang, and R. M. Arrieta, "Moth-inspired chemical plume tracing on an autonomous underwater vehicle," *IEEE Transactions on Robotics*, vol. 22, no. 2, pp. 292–307, 2006.
- [21] B. Luo, Q.-H. Meng, J.-Y. Wang, and M. Zeng, "A flying odor compass to autonomously locate the gas source," *IEEE Transactions on Instrumentation and Measurement*, vol. 67, no. 1, pp. 137–149, 2017.
- [22] S. Shigaki, T. Sakurai, N. Ando, D. Kurabayashi, and R. Kanzaki, "Time-varying moth-inspired algorithm for chemical plume tracing in turbulent environment," *IEEE Robotics and Automation Letters*, vol. 3, no. 1, pp. 76–83, 2017.
- [23] S. Shigaki, Y. Shiota, D. Kurabayashi, and R. Kanzaki, "Modeling of the adaptive chemical plume tracing algorithm of an insect using fuzzy inference," *IEEE Transactions on Fuzzy Systems*, vol. 28, no. 1, pp. 72–84, 2019.
- [24] G. Ferri, E. Caselli, V. Mattoli, A. Mondini, B. Mazzolai, and P. Dario, "Spiral: A novel biologically-inspired algorithm for gas/odor source

- localization in an indoor environment with no strong airflow,” *Robotics and Autonomous Systems*, vol. 57, no. 4, pp. 393–402, 2009.
- [25] F. Rahbar, A. Marjovi, P. Kibleur, and A. Martinoli, “A 3-d bio-inspired odor source localization and its validation in realistic environmental conditions,” in *2017 IEEE/RSJ International Conference on Intelligent Robots and Systems (IROS)*. IEEE, 2017, pp. 3983–3989.
  - [26] T. Lochmatter and A. Martinoli, “Tracking odor plumes in a laminar wind field with bio-inspired algorithms,” in *Experimental robotics*. Springer, 2009, pp. 473–482.
  - [27] P. Pyk, S. B. i Badia, U. Bernardet, P. Knüsel, M. Carlsson, J. Gu, E. Chanie, B. S. Hansson, T. C. Pearce, and P. F. Verschure, “An artificial moth: Chemical source localization using a robot based neuronal model of moth optomotor anemotactic search,” *Autonomous Robots*, vol. 20, no. 3, pp. 197–213, 2006.
  - [28] S. Pang and J. A. Farrell, “Chemical plume source localization,” *IEEE Transactions on Systems, Man, and Cybernetics, Part B (Cybernetics)*, vol. 36, no. 5, pp. 1068–1080, 2006.
  - [29] J.-G. Li, Q.-H. Meng, Y. Wang, and M. Zeng, “Odor source localization using a mobile robot in outdoor airflow environments with a particle filter algorithm,” *Autonomous Robots*, vol. 30, no. 3, pp. 281–292, 2011.
  - [30] J. A. Farrell, S. Pang, and W. Li, “Plume mapping via hidden Markov methods,” *IEEE Transactions on Systems, Man, and Cybernetics, Part B (Cybernetics)*, vol. 33, no. 6, pp. 850–863, 2003.
  - [31] M. V. Jakuba, “Stochastic mapping for chemical plume source localization with application to autonomous hydrothermal vent discovery,” Ph.D. dissertation, Massachusetts Institute of Technology, 2007.
  - [32] F. Rahbar, A. Marjovi, and A. Martinoli, “An algorithm for odor source localization based on source term estimation,” in *2019 International Conference on Robotics and Automation (ICRA)*. IEEE, 2019, pp. 973–979.
  - [33] M. Hutchinson, C. Liu, and W.-H. Chen, “Information-based search for an atmospheric release using a mobile robot: Algorithm and experiments,” *IEEE Transactions on Control Systems Technology*, vol. 27, no. 6, pp. 2388–2402, 2018.
  - [34] H. Jiu, Y. Chen, W. Deng, and S. Pang, “Underwater chemical plume tracing based on partially observable markov decision process,” *International Journal of Advanced Robotic Systems*, vol. 16, no. 2, p. 1729881419831874, 2019.
  - [35] S. Pang and F. Zhu, “Reactive planning for olfactory-based mobile robots,” in *2009 IEEE/RSJ International Conference on Intelligent Robots and Systems*. IEEE, 2009, pp. 4375–4380.
  - [36] L. Wang and S. Pang, “Chemical plume tracing using an auv based on pomdp source mapping and a-star path planning,” in *OCEANS 2019 MTS/IEEE SEATTLE*. IEEE, 2019, pp. 1–7.
  - [37] M. Vergassola, E. Villermanx, and B. I. Shraiman, “‘infotaxis’ as a strategy for searching without gradients,” *Nature*, vol. 445, no. 7126, p. 406, 2007.
  - [38] W. Naeem, R. Sutton, and J. Chudley, “Chemical plume tracing and odour source localisation by autonomous vehicles,” *The Journal of Navigation*, vol. 60, no. 2, pp. 173–190, 2007.
  - [39] N. Carpmann, “Turbulence intensity in complex environments and its influence on small wind turbines,” 2011.
  - [40] Q. Feng, H. Cai, Z. Chen, Y. Yang, J. Lu, F. Li, J. Xu, and X. Li, “Experimental study on a comprehensive particle swarm optimization method for locating contaminant sources in dynamic indoor environments with mechanical ventilation,” *Energy and buildings*, vol. 196, pp. 145–156, 2019.